Climate Shocks, Cyclones, and Economic Growth: Bridging the Micro-Macro Gap
Online Appendix

Laura Bakkensen
U. of Arizona

Lint Barrage
UCSB & NBER

October 2021

Contents

1 Empirical Analysis

1.1 Panel Regressions - Further Results

Table A0 presents summary statistics for each of our cyclone intensity measures ($\varepsilon_{j,t}$).

Table A0: Cyclone Intensity Measure Summary Statistics

Measure	Mean	Std. Dev.	Median	Min.	Max.
#Landfalls$_t$	.31611	1.2663	0	0	16
#Landfalls$_t$/sqkm	.00003	.00076	0	0	.071429
Max. Wind Speed$_t$ (knots)	6.1461	19.860	0	0	150
Max. Wind Speed$_t$ (knots)/sqkm	.00119	.02436	0	0	1.97282
Energy†/sqkm	.00680	.16315	0	0	11.3439

†Energy is sum of maximum wind speeds cubed divided by 1000.

Table A1 presents output growth panel specification (1) using cyclone *energy* as intensity metric.

Table A1: Panel Analysis: Cyclone Strikes and Growth - Energy/sqkm

Dependent Variable:	Real GDP/Capita Growth$_{j,t}$					
Sample:	Unfiltered			Has Controls		
	(1)	(2)	(3)	(4)	(5)	(6)
Energy/sqkm$_{j,t}$	-0.004	-0.208***	-0.583***	-0.074***	-0.241***	0.191
	(0.010)	(0.059)	(0.040)	(0.010)	(0.073)	(0.493)
Credit$_{j,t}$·(Energy/sqkm$_{j,t}$)		0.002***			0.002***	
		(0.001)			(0.001)	
ln (GDP p.c.)$_{j,t-1}$·(Energy/sqkm$_{j,t}$)			0.059***			-0.026
			(0.004)			(0.049)
Domestic Credit$_{j,t}$		-0.000			-0.000**	
		(0.000)			(0.000)	
ln (GDP p.c.)$_{j,t-1}$			-0.103***			-0.219***
			(0.013)			(0.033)
Country F.E.s:	Yes	Yes	Yes	Yes	Yes	Yes
Year F.E.s:	Yes	Yes	Yes	Yes	Yes	Yes
Country-Trends:	Yes	Yes	Yes	Yes	Yes	Yes
S.E. Cluster	Country	Country	Country	Country	Country	Country
Observations	7,573	5,690	7,573	1,978	1,978	1,978
#Countries	182	171	182	116	116	116
Adj. R-Squared	0.110	0.102	0.167	0.178	0.201	0.278

Table presents regression of countries' real GDP per capita growth rate in year t on cyclone energy (sum of max. wind speeds cubed/1000 and normalized by land area) in year t plus controls for lagged natural log of real GDP per capita in level and interacted with energy (Cols. 3, 6) or domestic credit provided by financial sector (%GDP) in level and interacted with energy (Cols. 2, 5). All regressions include country fixed effects, year fixed effects, country-specific linear time trends, and a constant. Standard errors are heteroskedasticity-robust and clustered at the country level. (*** p<0.01, ** p<0.05, * p<0.1).

Table A2 compares key properties of countries included in the "unfiltered" sample versus the sample with rich macroeconomic control variables as considered in paper Table 1. The results indicate that countries with standard control variables have, on average, significantly larger populations, higher statistical capacity, and less volatile growth.

Table A2: Sample Comparison

		Sample		
		"Unfiltered"	"Has Controls"	Diff. (SE)
Population	Mean	31.1	49.1	-18.0 (3.40)***
Statistical Capacity Rating	Mean	68.2	74.2	-6.0 (0.70)***
Real GDP p.c. Growth	Mean	1.8%	2.2%	-0.4% (0.12)**
	Var.	6.7%	4.2%	f = 2.53***

Table compares means or variance for indicated variables across "Unfiltered" and "Has Controls" samples of country-years. Means are compared with two-sided t-tests (with Welch approximation for unequal variances). Variance compared with F-test. (*** p<0.01, ** p<0.05, * p<0.1).

1.2 Cross-Sectional Regressions

This section describes our implementation of a cross-sectional analysis of cyclone risk and economic growth in the spirit of Skidmore and Toya (2002) within our harmonized global panel. Skidmore and Toya (2002) regresses countries' average 1960-90 growth rates on disaster metrics such as the average number of climatic events per year in a sample of 89 countries. One potential concern about Skidmore and Toya's (2002) analysis is that they use countries' reported disaster occurrences in EMDAT to measure general disaster risk, which are subject to several inclusion criteria and thus constitute a partly selected sample. We regress each country $j's$ average growth rate from 1970-2015 ($\overline{g}_j$) on different meteorological cyclone risk measures ($\mu_{\varepsilon,j}$) and a host of control variables ($\mathbf{X_j}$), including the fraction of land area in the tropics, absolute latitude, the fraction of the population living within 100 kilometers of navigable water, an institutional quality proxy, and initial GDP per capita.[1]

$$\overline{g}_j = \beta_0 + \beta_1 \mu_{\varepsilon,j} + \mathbf{X_j}'\boldsymbol{\beta} + \epsilon_j \tag{1}$$

Table A3 presents the results. Column (1) confirms that a significant positive correlation between economic growth and Skidmore and Toya's main disaster risk measure, the natural logarithm of disaster counts (per land area), survives in our extended global sample using modern meteorological data, although this effect appears non-monotonic (Columns (2) and (4)). The positive association

[1] We calculate the fraction of a country's population residing within 100 kilometers of navigable water (defined as a coast, major river, or major lake) in ArcGIS using geospatial shoreline data from the U.S. National Oceanic and Atmospheric Administration's Global Self-consistent, Hierarchical, High-resolution Geography Database and population data from the Gridded Population of the World v4 produced by the Center for International Earth Science Information Network at Columbia University and as published through the Socioeconomic Data and Applications Center. We calculate in ArcGIS the fraction of a country's land area in a tropical climate zone based on Köppen-Geiger climate classification maps provided by Rubel and Kottek (2010). Institutional quality is proxied by the Transparency International Corruption Perceptions Index.

between cyclone risk and growth is also attenuated through the inclusion of controls for savings and human capital accumulation (Columns (3) and (5)),[2] consistent with the possibility that higher savings and human capital investment rates could be part of the underlying mechanism driving the positive association between risk and growth. Of course it is important to note that these results are ultimately only suggestive, however, as cross-sectional growth regressions likely suffer from omitted variable bias. Indeed, our quantitative model does not project positive impacts of cyclone risk on growth in any of the countries we consider.

Table A3: Cross-Sectional Cyclone Risk and Growth Association

Dependent Variable:	Avg. Real GDP/Capita Growth $\overline{g}_{1970-2015,j}$				
$\overline{\text{Cyclones}_j}$ Measure:	$\ln(\frac{\text{Landfalls}}{\text{sqkm}})$	Landfalls/sqkm		Max. Wind/sqkm	
	(1)	(2)	(3)	(4)	(5)
$\overline{\text{Cyclones}_j}$	0.100***	185.934**	135.233	7.077**	5.765
	(0.032)	(76.478)	(93.210)	(3.516)	(3.565)
$(\overline{\text{Cyclones}_j})^2$		-6,470.275**	-6,647.325*	-11.266**	-11.733*
		(2,695.255)	(3,999.375)	(5.562)	(6.281)
$\overline{\text{SavingsRate}_j}$			0.093***		0.092***
			(0.022)		(0.022)
$\overline{\text{YearsSchooling}_j}$			0.009		0.020
			(0.064)		(0.063)
Tropics (%Area)	-0.009*	-0.011**	-0.008	-0.010**	-0.007
	(0.005)	(0.005)	(0.005)	(0.005)	(0.005)
Abs. Latitude	-0.015	-0.021	-0.017	-0.021	-0.016
	(0.013)	(0.014)	(0.014)	(0.014)	(0.014)
Water Proximity (%Area)	0.001	0.004	0.012***	0.004	0.013***
	(0.005)	(0.005)	(0.005)	(0.005)	(0.005)
Institutions (CPI_{2015})	0.030***	0.035***	0.016*	0.035***	0.015
	(0.009)	(0.009)	(0.009)	(0.009)	(0.009)
Initial GDP/Cap.$_{1970}$	-0.025***	-0.027***	-0.044***	-0.027***	-0.044***
	(0.003)	(0.003)	(0.006)	(0.003)	(0.006)
Observations	131	132	113	132	113
Adj. R-Squared	0.303	0.274	0.392	0.261	0.398

Table presents OLS regression of countries' avg. real GDP per capita growth rate (1970-2015) on natural log of avg. number of cyclone landfalls per year +0.0000001 normalized by area (Col. 1), the avg. number of landfalls per year normalized by area in levels (Cols. 2, 3) and squared (Col. 3), or avg. max. sustained wind speed per year normalized by area in levels (Cols. 4, 5) and squared (Col. 5). All specifications control for the share of land area in the tropics, absolute value of latitude, fraction of pop. within 100km of major river, lake, or coast, the Transparency International Corruption Perceptions Index, 1970 GDP/capita in $1000s, and a constant. Cols. (3) and (5) further control for avg. savings rates and avg. years of schooling. Standard errors are heteroskedasticity-robust and presented in parentheses (*** p<0.01, ** p<0.05, * p<0.1).

[2] Educational attainment estimates are from Barro and Lee (2012).

2 Theoretical Derivations

2.1 Stationary Equilibrium Growth

This section derives the paper's equations defining equilibrium growth (10), following the approach in Krebs (2003a,b). Country subscripts j are omitted for legibility. First, note that the household's problem can be written in recursive form as:

$$V(w, \widetilde{k}, \varepsilon) = \max u(c) + \beta E[V(w', \widetilde{k}', \varepsilon')] \tag{2}$$

subject to:

$$w' = w[1 + r(\widetilde{k}, \varepsilon)] - c \tag{3}$$

where $r(.)$ is as defined in paper equation (6). Substituting (3) into (2) and taking the first-order conditions for c and $\widetilde{k}'$ yields:

$$\begin{aligned} u'_c &= \beta E[V'_{w'}] \\ 0 &= \beta E[V'_{\widetilde{k}'}] \end{aligned} \tag{4}$$

Next, substituting in the decision rules $c = g(w, \widetilde{k}, \varepsilon)$ and $\widetilde{k}' = f(w, \widetilde{k}, \varepsilon)$ yields the Benveniste-Scheinkman conditions:

$$\begin{aligned} V'_w &= \beta E[V'_{w'}[(1 + r(\widetilde{k}, \varepsilon)]] \\ V'_{\widetilde{k}} &= \beta E[V'_{w'} w (1 + \widetilde{k})^{-2} \left\{ [R^k(\widetilde{k}, \varepsilon) - \delta_k - \eta^k(\varepsilon)] - [R^h(\widetilde{k}, \varepsilon) - \delta_k - \eta^h(\varepsilon)] \right\}] \end{aligned}$$

Substituting based on (4) and iterating forward then yields the Euler equation and asset allocation optimality condition, respectively:

$$u'_c = \beta E[u'_{c'}[(1 + r(\widetilde{k}', \varepsilon')]] \tag{5}$$

$$0 = \beta E[u'_{c'} \frac{w'}{(1 + \widetilde{k}')} \left\{ [R^k(\widetilde{k}', \varepsilon') - \delta_k - \eta^k(\varepsilon')] - [R^h(\widetilde{k}', \varepsilon') - \delta_h - \eta^h(\varepsilon')] \right\}] \tag{6}$$

Next, invoking the assumed utility function $u(c) = \frac{c^{1-\gamma}}{1-\gamma}$, the budget constraint (3), and the fact that $c' = \widetilde{c}[1 + r(\widetilde{k}', \varepsilon')]w'$ (where $\widetilde{c} \equiv 1 - \widetilde{s}$ denotes the consumption-out-of-wealth ratio), substitution and rearranging in (5) yields the desired result that:

$$\widetilde{s} = 1 - \widetilde{c} = \left(\beta E[(1 + r(\widetilde{k}', \varepsilon'))^{1-\gamma}] \right)^{\frac{1}{\gamma}} \tag{7}$$

The same substitutions allow us to factor out as pre-determined terms $\widetilde{c}$ and $w' = (1 + r)w - c$ in (6). Further noting that, in stationary equilibrium, $\widetilde{k}' = \widetilde{k}$, we obtain the desired condition:

$$0 = \beta E[\frac{\left\{ [R^k(\widetilde{k}', \varepsilon') - \delta_k - (1 - \pi)\eta^k(\varepsilon')] - [R^h(\widetilde{k}', \varepsilon') - \delta_k - (1 - \pi)\eta^h(\varepsilon') \right\}}{(1 + r(\widetilde{k}', \varepsilon'))^{\gamma}}] \tag{8}$$

Finally, the expression for average growth can be derived by again invoking $w' = [1 + r(\widetilde{k}, \varepsilon)]w - c$ and $c' = \widetilde{c}[1 + r(\widetilde{k}', \varepsilon')]w'$. First, note that the definition of $\widetilde{c}$ implies that:

$$\begin{aligned} \widetilde{c} &= \frac{c}{[1 + r(\widetilde{k}, \varepsilon)]w} \\ &\rightarrow \quad 1 - \widetilde{c} = \frac{[1 + r(\widetilde{k}, \varepsilon)]w - c}{[1 + r(\widetilde{k}, \varepsilon)]w} \end{aligned} \tag{9}$$

Consequently, expected growth can readily be shown to equal paper equation (10), as desired:

$$\begin{aligned} E\left[\frac{c'}{c}\right] &= E\left[\frac{\widetilde{c}[1 + r(\widetilde{k}', \varepsilon')]w'}{c}\right] = E\left[\frac{\widetilde{c}[1 + r(\widetilde{k}', \varepsilon')]\{[1 + r(\widetilde{k}, \varepsilon)]w - c\}}{c}\right] \\ &= (1 - \widetilde{c})(1 + E[r(\widetilde{k}', \varepsilon')]) = (\widetilde{s})(1 + E[r(\widetilde{k}', \varepsilon')]) \end{aligned} \tag{10}$$

2.2 Storm Risk Impacts

This section substantiates the claim that *cyclone realizations have a negative effect on contemporaneous growth ($\frac{dg_t}{d\varepsilon_t} < 0$)* in our model. This claim follow from the equation for realized growth in stationary equilibrium (19) with the definition of portfolio returns (15) substituted in:

$$\begin{aligned} g_t &= \frac{c_t}{c_{t-1}} = (\widetilde{s})[1 + \omega_k(\widetilde{k})\{R^k(\widetilde{k}, \varepsilon_t) - \overline{\delta^k} - (1 - \pi)\eta^k(\varepsilon_t)\} \\ &\quad + (1 - \omega_k(\widetilde{k}))\{R^h(\widetilde{k}) - \overline{\delta^h} - (1 - \pi)\eta^h(\varepsilon_t)\}] \end{aligned} \tag{11}$$

Differentiating (11) with respect to cyclone realizations yields:

$$\begin{aligned} &\frac{dg_t}{d\varepsilon_t} \\ &= (\widetilde{s})(1 - \pi)\left[\omega_k(\widetilde{k})\{\frac{\partial R^k(.)}{\partial \varepsilon_t} - \frac{\partial \eta^k(.)}{\partial \varepsilon_t}\} + (1 - \omega_k(\widetilde{k}))\{\frac{\partial R^h(.)}{\partial \varepsilon_t} - \frac{\partial \eta^h(.)}{\partial \varepsilon_t}\}\right] < 0 \end{aligned} \tag{12}$$

where the inequality follows from the definition of factor returns (14) and our assumptions about the damage functions as increasing in cyclone intensity.

3 Model Quantification

3.1 TFP - Further Results

3.1.1 Varying Lag Lengths

Table A4 present TFP impacts across varying cyclone lag lengths, along with Akaike/Bayesian Information Criteria (AIC/BIC). The results are generally similar across lag lengths, but cease to be precisely estimated as more observations are excluded at higher lag lengths. The information criteria also imply that lower lag lengths are preferred.

Table A4: Benchmark TFP Impacts at Varying Lag Lengths: Max Wind/sqkm

MaxWind_t	-1.485*	-1.661*	-1.951*	-2.069*	-2.061*	-2.345	-2.286	-2.406	-2.649	-2.922
	(0.859)	(0.948)	(1.111)	(1.201)	(1.171)	(1.500)	(1.460)	(1.558)	(1.696)	(1.946)
MaxWind_{t-1}		-1.569**	-1.856**	-1.995*	-2.095*	-2.158*	-2.382*	-2.496	-2.757	-2.601
		(0.734)	(0.892)	(1.013)	(1.082)	(1.157)	(1.429)	(1.539)	(1.710)	(1.749)
MaxWind_{t-2}			-1.899*	-2.035*	-2.129*	-2.263*	-2.280	-2.503	-2.770	-2.612
			(1.009)	(1.132)	(1.207)	(1.353)	(1.395)	(1.643)	(1.822)	(1.877)
MaxWind_{t-3}				-1.704	-1.821	-1.982	-2.080	-2.147	-2.648	-2.500
				(1.156)	(1.241)	(1.389)	(1.473)	(1.504)	(1.941)	(1.946)
MaxWind_{t-4}					-1.497*	-1.646	-1.771	-1.845	-2.095	-2.316
					(0.889)	(1.039)	(1.170)	(1.245)	(1.373)	(1.737)
MaxWind_{t-5}						-1.877	-1.988	-2.112	-2.306	-2.266
						(1.225)	(1.370)	(1.500)	(1.642)	(1.755)
MaxWind_{t-6}							-1.588	-1.704	-1.982	-1.778
							(1.002)	(1.163)	(1.379)	(1.439)
MaxWind_{t-7}								-1.584	-1.834	-1.705
								(0.999)	(1.240)	(1.341)
MaxWind_{t-8}									-1.927	-1.720
									(1.166)	(1.256)
MaxWind_{t-9}										0.955
										(1.288)
Obs.	6,161	6,033	5,905	5,777	5,649	5,521	5,393	5,265	5,137	5,009
Adj. R^2	0.642	0.639	0.635	0.631	0.625	0.618	0.610	0.602	0.594	0.588
AIC	-8447	-8386	-8327	-8255	-8160	-8067	-7968	-7898	-7813	-7722
BIC(n=#Clusters)	-8316	-8255	-8197	-8124	-8029	-7936	-7837	-7767	-7682	-7591

Regression of log benchmark TFP $\ln(A_{jt})$ on a constant, country fixed-effects, year fixed-effects, country-specific linear time trends, and cyclones (max. wind speed/sqkm) for various lags. Standard errors are heterosk.-robust and clustered at the country level.

3.1.2 Robustness: HP Filtering and Cyclone Energy

This section presents two robustness analyses for our cyclone strike impact estimates on TFP. First, Table A5 Column 1 shows results for cyclone impacts on TFP based on HP-filtering of each country's TFP series as opposed to log-linear detrending in the benchmark. We use an annual smoothing parameter $\lambda = 6.25$ and regress the natural logarithm of the cyclical components, $\ln(\widetilde{TFP}_{j,t})$ on year fixed-effects and cyclone measures $\varepsilon_{j,t}$ (equal to either maximum wind speed per square kilometer or energy per square kilometer), with robust errors $\epsilon_{j,t}$ clustered at the country-level:

$$\ln(\widetilde{TFP}_{j,t}) = \delta_t + \sum_{l=0}^{L} \beta_{1+l}^{A} \varepsilon_{j,t-l} + \epsilon_{j,t}$$

In line with the benchmark results, we find significant negative effects of cyclone strikes on (cyclical) TFP (Column 1). Second, Table A5 also presents results analogous to main paper Table 1 but using cyclone *energy* (maximum wind speeds cubed summed over the lifetime of a storm over a given country) per square kilometer - rather than maximum wind speeds per square kilometer - as cyclone intensity measure. While the point estimates continue to suggest negative TFP impacts that last for several periods, these estimates are generally imprecise (perhaps due to the additional weight given to outliers by the energy measure).

Table A5: HP-Filtering and Cyclone Energy

	(1)	(2)
Cyclone Measure:	Max Wind / sqkm	Energy / sqkm
$\varepsilon_{j,t}$	-52.971***	-0.244*
	(8.380)	(0.126)
$\varepsilon_{j,t-1}$	-27.829***	-0.074
	(8.228)	(0.157)
$\varepsilon_{j,t-2}$	-15.826*	-0.190
	(8.696)	(0.187)
$\varepsilon_{j,t-3}$	4.037	-0.090
	(10.628)	(0.166)
$\varepsilon_{j,t-4}$	-1.276	0.153
	(7.161)	(0.228)
Obs.	2,812	5,649
Clusters	144	144
Adj. R^2	0.0651	0.625

Table presents regression of natural log of cyclical component of TFP (based on HP-filtering, with $\lambda = 6.25$) on a constant, year fixed-effects, and cyclone intensity up to four lags, measured either by max. wind speed/km^2 (Col. 1) or cyclone energy (sum of maximum wind speeds cubed/1000 km^2 (Col. 2). Standard errors are heteroskedasticity-robust and clustered at country level. *** $p<0.01$, ** $p<0.05$, * $p<0.1$.

3.2 Physical and Human Capital Losses - Further Results

Table A6 presents a robustness check for the depreciation impact estimation in paper Table 3 but using damage data from MunichRe instead of EMDAT (as aggregated to the country-year level for tropical cyclones and made available by Neumayer, Plumber, and Barthel (2014)).

Table A6: Capital Losses Robustness: MunichRe (Neumayer et al., 2014) Damage Data

Dependent Variable:	$\ln(\text{PropertyDamages}_{j,t}/K_{j,t})$			
	(1)	(2)	(3)	(4)
$\ln(\text{MaxWind}_{j,t})$	3.568***	5.945***	0.976	1.053
	(0.412)	(1.062)	(0.765)	(0.758)
$\ln(\text{MaxWind}_{j,t})\cdot \ln(\text{GDP pc})_{j,t-1}$			-0.039	-0.067
			(0.085)	(0.085)
$\ln(\text{MaxWind}_{j,t})\cdot(\text{Pct. Below 5m})_{j,t}$				0.020**
				(0.008)
$\ln(\text{GDP pc})_{j,t-1}$			-0.627	-0.919
			(0.832)	(0.838)
$\text{Pct. Below 5m}_{j,t}$				0.207***
				(0.068)
Constant	22.384***	59.324***	1.281	1.951
	(3.740)	(12.199)	(7.469)	(7.424)
Country Fixed Effects?	Yes	U.S. Only	No	No
Observations	320	27	320	320
Adj. R-Squared	0.196	0.602	0.169	0.190

Table presents regression of natural log of fractions of capital stock destroyed (Cols. 1-4) on natural log of $\text{MaxWind}_{j,t}$ (max. wind speed normalized by country area), lagged GDP per capita levels and max. wind interactions (Cols. 3, 4), the percentage of population living below 5 meters elevation in levels and max. wind interactions (Col. 4), and country fixed-effects (Col 1). Col. 2 restricts sample to U.S. storms only. Damages based on Neumayer et al. (2014) aggregates of MunichRe data. Heteroskedasticity-robust standard errors in parentheses (*** p<0.01, ** p<0.05, * p<0.1).

4 Cyclone Risk Quantification

4.1 Cyclone Intensity Monte Carlo Simulation Details

First, we use the Emanuel et al.'s (2008) cyclone frequency data to estimate the projected mean number of storms making landfall in each country j under the future climate T_{2090}. Next we assume a Poisson distribution of cyclone counts (Emanuel, 2013) to randomly sample the *number* of storms making landfall in each country j per year under the future climate (taking $n = 5,000$ draws from the Poisson$(\#landfalls_j|T_{2090})$ distribution for each country j). Third, for each draw of a *number* of storms making landfall in country j, we then randomly sample (with replacement) maximum wind speed from one of the 3,000 synthetic tracks per basin (5,000 tracks in the North Atlantic Ocean) in the Emanuel data. This process thus generates random draws over *annual* cyclone realizations, including years without storms. This process captures changes in expected

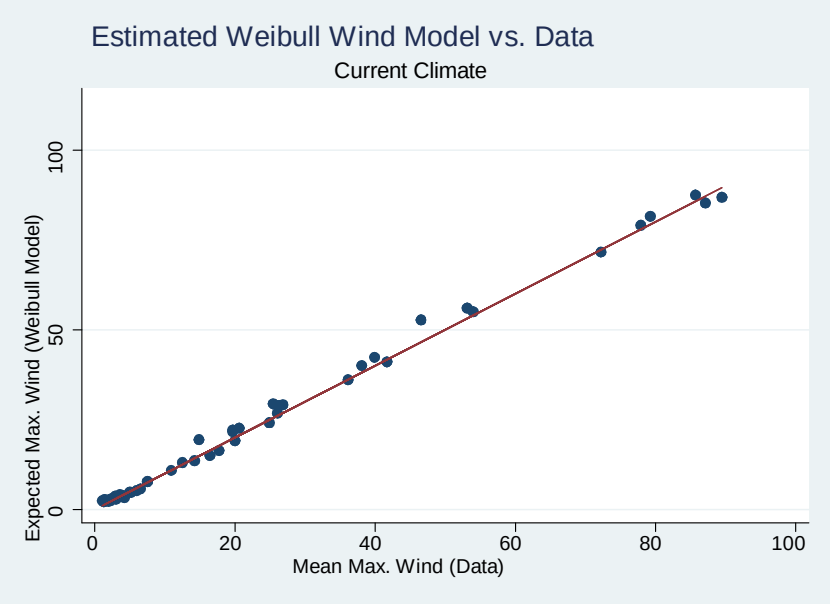

Figure 1: Figure A1: Estimated Weibull Expected Wind Speeds vs. Data

future intensity driven both by changes in the number and characteristics of storms. Finally, we then fit Weibull distributions for each country.

In order to validate our approach, Figure A1 compares the estimated Weibull model's expected annual maximum wind speeds for each country under the current climate against their empirically observed mean maximum wind speeds in the data. The model appears to fit the data very well, with a correlation coefficient of 0.9982.

4.2 Cyclone Risk Changes

Figures A2 and A3 showcase our model's benchmark projected changes in cyclone risk for each country, specifically by plotting each country's current mean annual maximum wind speed per square kilometer (x-axis) against each country's expected end-of-century (2100) annual mean maxmimum wind speed per square kilometer. Figure A2 shows results for the full sample of countries for which we quantify the model, whereas Figure A3 zooms in to better display predicted changes for countries whose future expected risk is less than 0.003 knots per square kilometer.

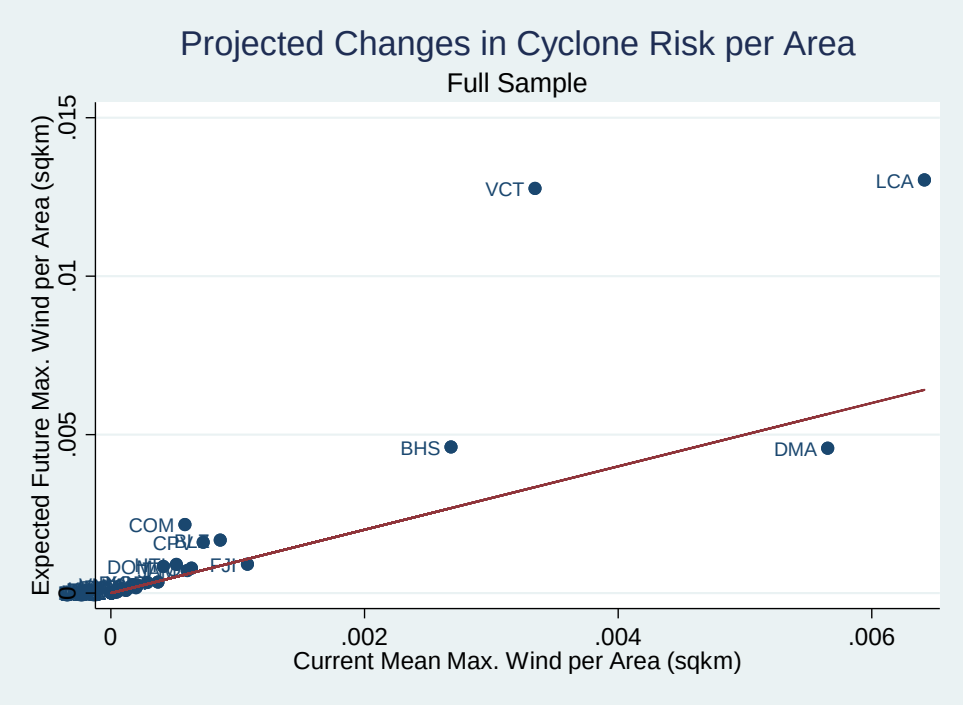

Figure A2: Current Mean vs. Future Expected Max. Wind Speed per Area

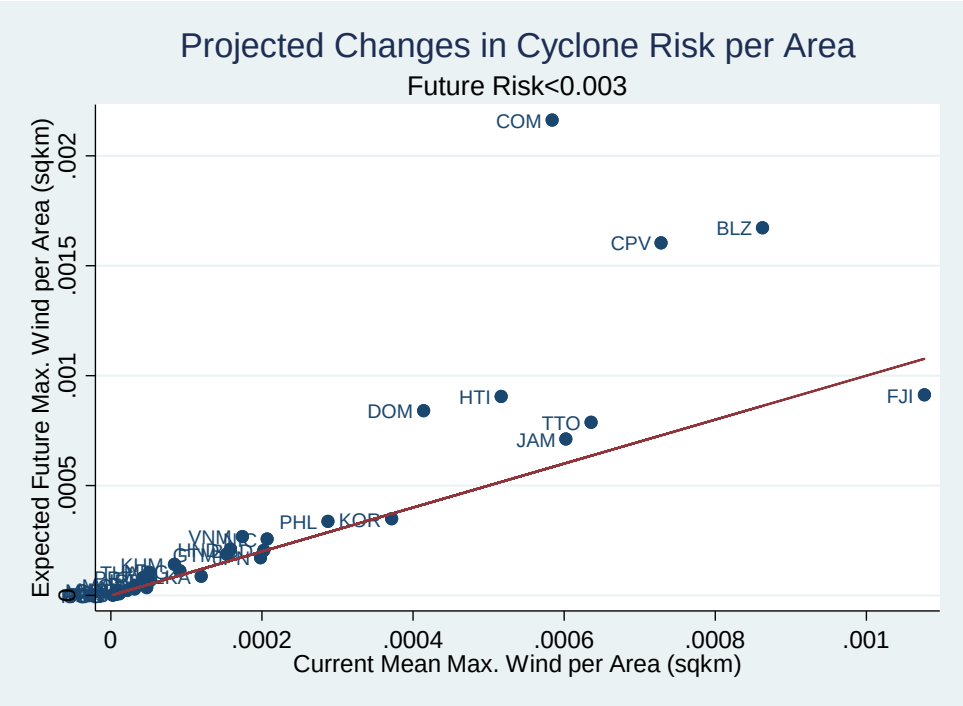

Figure A3: Current Mean vs. Future Expected Max. Wind Speed per Area (Zoomed In)

4.3 Country Codes

Table A7 presents the country code-name matching pertinent to our graphs.

5 Quantitative Model

5.1 Further Model Assessment Results

First, Figure A4 shows the correlation between the predicted contemporaneous output growth impacts for a hypothetical Category 5 hurricane based on our structural model (y-axis) and the empirical results in Table 1 Column 2 (for maximum wind speed per square kilometer). The results are very similar to the ones using Table 1 Column 6 to quantify empirical impact predictions.

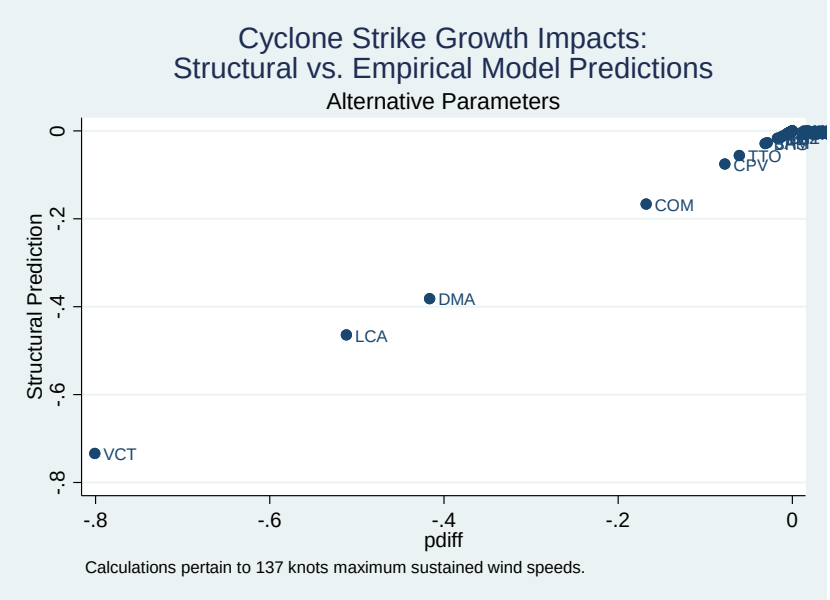

Figure 2: Figure A4: Structural Model vs. Emprical Predictions of Cyclone Strike Impacts

Second, we evaluate the dynamics of predicted cyclone impacts in each country over time in order to verify that the predicted output losses are persistent. Figures A5 and A6 showcase two examples of the predicted output dynamics with and without a cyclone strike in period 2 (after year 2014 baseline conditions). As expected, output falls as a result of the storm. This decline in output also lowers investment in the year of the storm, which, in turn, lowers output (relative to the counterfactual) in the subsequent year and beyond. The magnitude of the relative output loss is mitigated in the years after the storm as TFP losses are assumed (in the shown simulations) to be short-lived. However, the impacts on output due to lower capital stocks are persistent.

Table A7: Country Codes

Code	Country
AUS	Australia
BGD	Bangladesh
BHS	Bahamas, The
BLZ	Belize
CAN	Canada
CHN	China
COL	Colombia
COM	Comoros
CPV	Cabo Verde
DMA	Dominica
DOM	Dominican Republic
FJI	Fiji
GBR	United Kingdom
GTM	Guatemala
HND	Honduras
HTI	Haiti
IDN	Indonesia
IRL	Ireland
JAM	Jamaica
JPN	Japan
KHM	Cambodia
KOR	Korea, Rep.
LCA	St. Lucia
LKA	Sri Lanka
MDG	Madagascar
MEX	Mexico
MMR	Myanmar
MOZ	Mozambique
MYS	Malaysia
NIC	Nicaragua
NZL	New Zealand
PAK	Pakistan
PHL	Philippines
PRT	Portugal
RUS	Russian Federation
THA	Thailand
TTO	Trinidad and Tobago
USA	United States
VCT	St. Vincent and the Grenadines
VNM	Vietnam

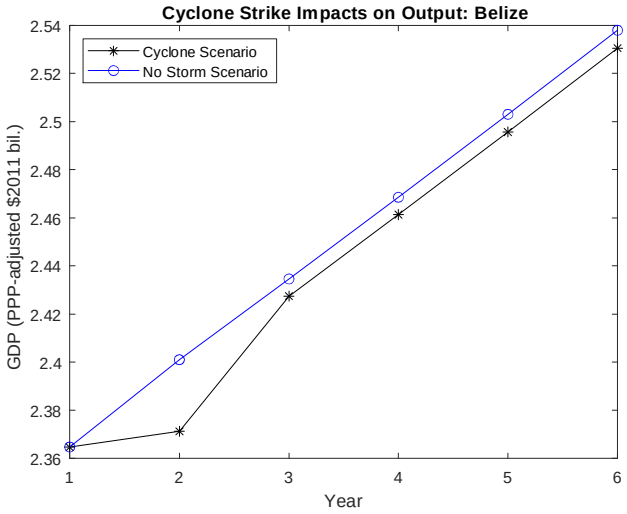

Figure A5: Cyclone Strike Impact Simulation - Belize

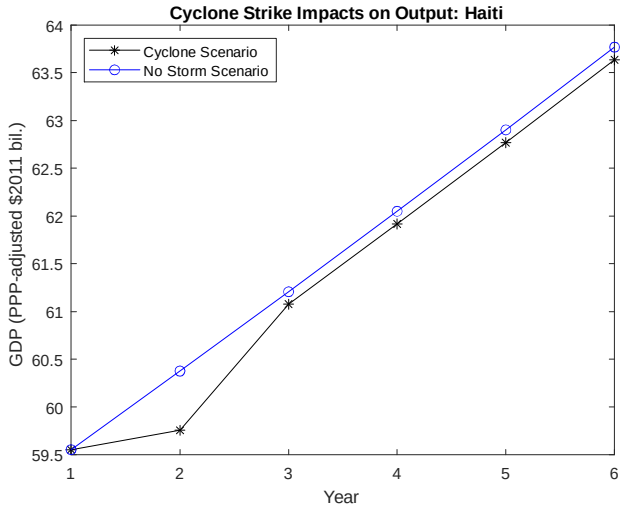

Figure A6: Cyclone Strike Impact Simulation - Haiti

π

5.2 Counterfactual Results: Robustness

5.2.1 Matched Savings Rates

We seek to compare our model's predicted savings rates to the data by comparing the model's projected physical capital investment rates (x_k/Y_t) to gross fixed capital formation as a percentage of GDP in the data (Penn World Tables) for the model base year of 2014. While the model's predictions are quantitatively reasonable, ranging from 20.2% to 26.9%, they do not correlate well with variation in gross fixed capital formation rates in the data. This is arguably not surprising

as our model, designed to capture marginal changes in investment rates due to variation in storm risks, abstracts from other determinants of investment rate levels, such as age dependency ratios, fiscal policy, pension systems, capital controls, etc. In order to assess the robustness of the results to this issue, we implement an alternative version of the model which allows utility discount factors β_j to vary across countries and forces the calibration to match capital investment rates from the data. More formally, the revised calibration selects the base year values for $\widetilde{s_{0,t}}$, $\widetilde{k_{0,j}}$, initial TFP level $\overline{A_{0,j}}$ and utility discount factor β_j to jointly match (i) the base year output growth rate in the data, (ii) the base year capital investment rate in the data (as the equilibrium $x^*_{k,j,t}/Y_{j,t}$ in the model), (iii) capital allocation optimality condition (paper equation 9), and (iv) the Euler equation (paper equation 8) for each country. The central drawback of this approach is that allowing flexibility in β_j is not enough to match the investment rates observed in some countries, which we consequently have to drop from the analysis. For example, matching China's high savings rate would require a β in excess of unity.

Table A8 below lists the β_j values and gross capital formation rates that we match in this alternative model versio. Figures A7 and A8 showcase results for the welfare and growth impacts of cyclone risk changes in this setting, respectively (analogous to main paper Figures 5 and 6). While the estimated welfare impacts are broadly similar as in the benchmark, they do increase for countries with higher utility discount factors than the benchmark calibration value of $\beta = 0.975$ (e.g., the Bahamas), and decrease for countries with lower utility discount factors than in the benchmark (e.g., the United States). The estimated growth impacts are, however, virtually identical, with a correlation of 0.98 across the the benchmark and 'matched savings rates' version of the model.

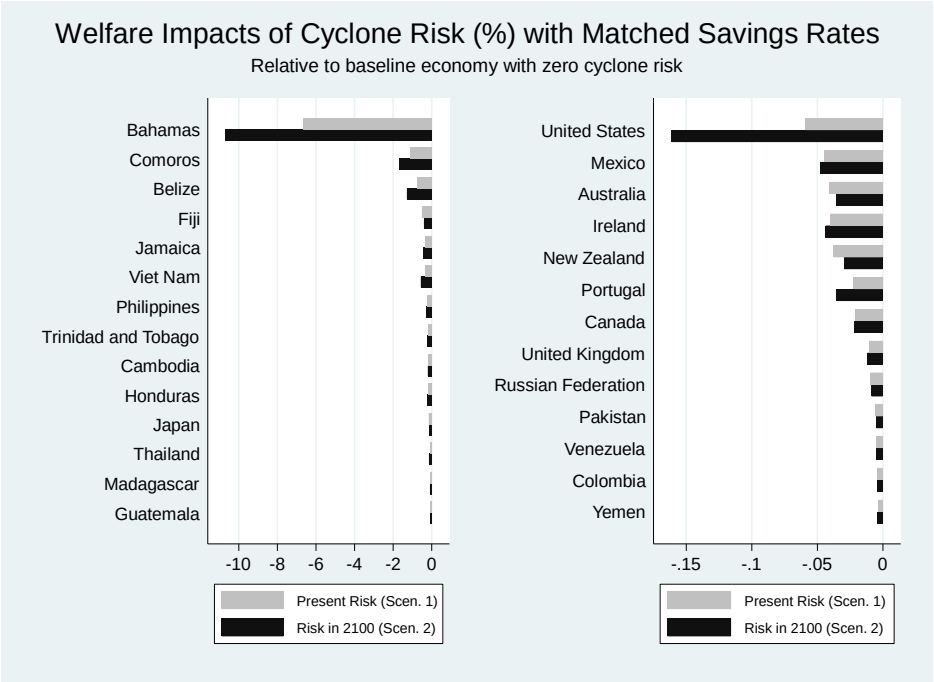

Figure A7: Welfare Impacts of Cyclone Risk in Model with Matched Savings Rates

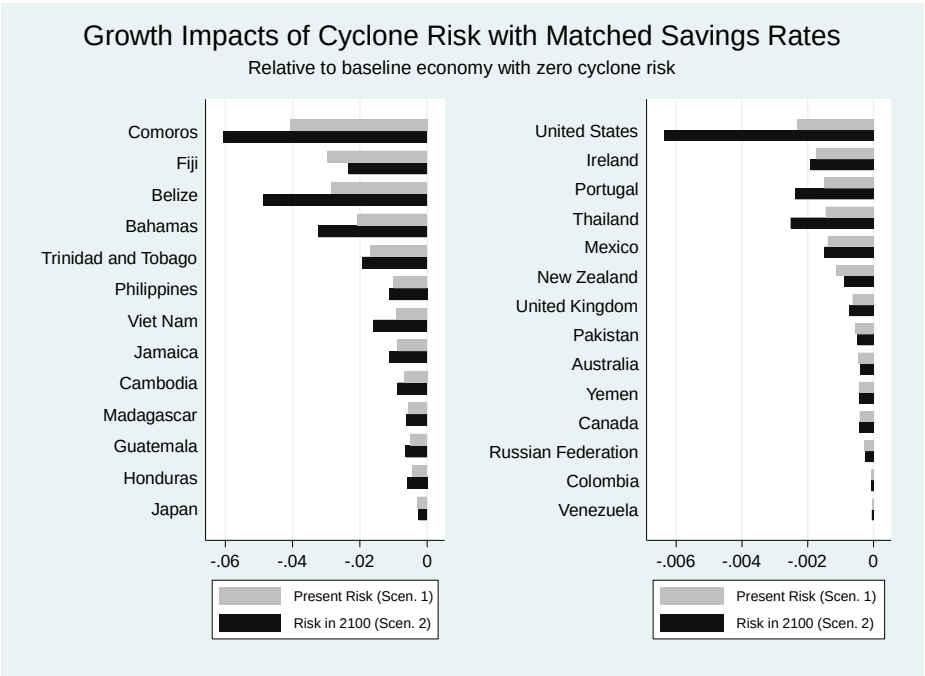

Figure A8: Growth Impacts of Cyclone Risk in Model with Matched Savings Rates

Table A8: Matched Savings Rates Calibration

Country	Gross Capital Formation (%GDP)	Beta
Australia	27	0.989
Bahamas	32	0.990
Belize	21	0.942
Cambodia	22	0.971
Canada	25	0.976
Colombia	26	0.999
Comoros	27	0.937
Fiji	19	0.926
Guatemala	14	0.877
Honduras	22	0.963
Ireland	22	0.969
Jamaica	22	0.954
Japan	24	0.964
Madagascar	15	0.889
Mexico	22	0.950
New Zealand	23	0.967
Pakistan	15	0.863
Philippines	21	0.964
Portugal	15	0.894
Russian Federation	22	0.951
Thailand	24	0.971
Trinidad and Tobago	13	0.864
United Kingdom	17	0.912
United States	20	0.943
Venezuela	25	0.922
Vietnam	27	0.993
Yemen	8	0.784

5.2.2 Alternative Climate Models

The benchmark results are based on emissions scenarios processed through the GFDL general circulation model (Manabe et al., 1991). Figure A9 showcases the robustness of the results to three alternative climate models used by Emanuel (2008) and Emanuel et al. (2008). While the GFDL model does predict future risk increases which can be both noticeably higher (e.g., the United States) and lower (e.g., Fiji, Bangladesh) than other models, the results are mostly similar across models within each country.

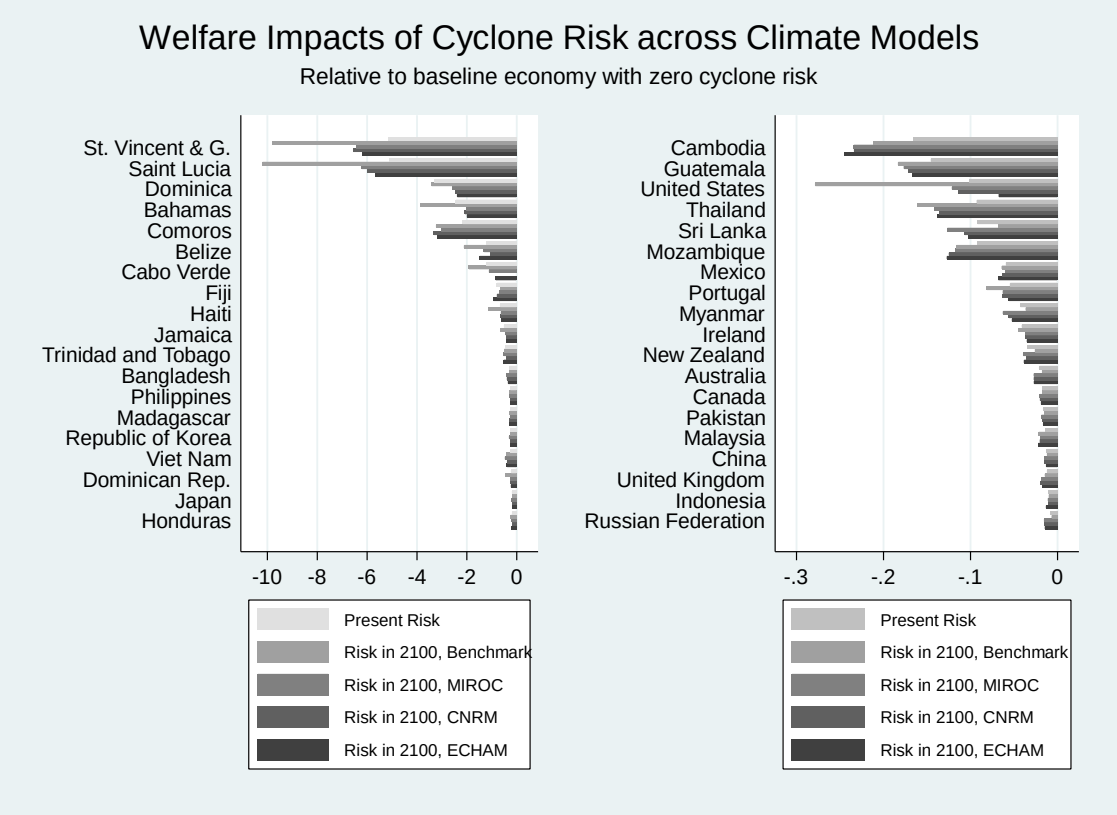

Figure A9: Welfare Impacts of Cyclone Risk across Climate Models

5.3 Indirect Impacts: Mechanisms

Finally, this section highlights some of the mechanisms in our paper through which households respond to cyclone risk. Figure A10 showcases that our benchmark model calibration implies that countries' savings rates $\widetilde{s}_j$ are increasing in cyclone risk (measured by expected maximum wind speeds per square kilometer). Figure A11 shows that countries' propensity to invest in physical over human capital is decreasing in cyclone risk.

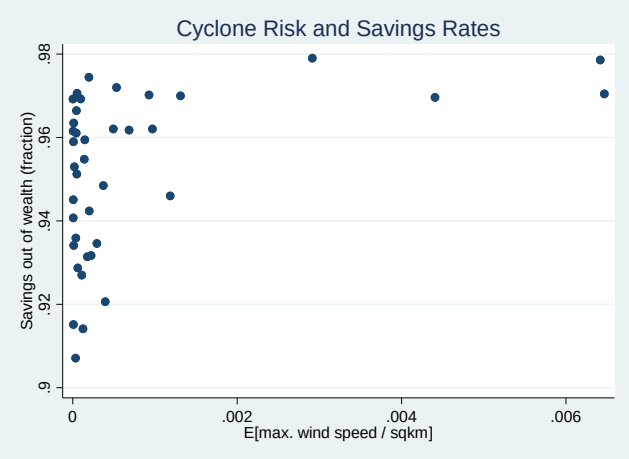

Figure A10: Cyclone Risk and Savings Rates

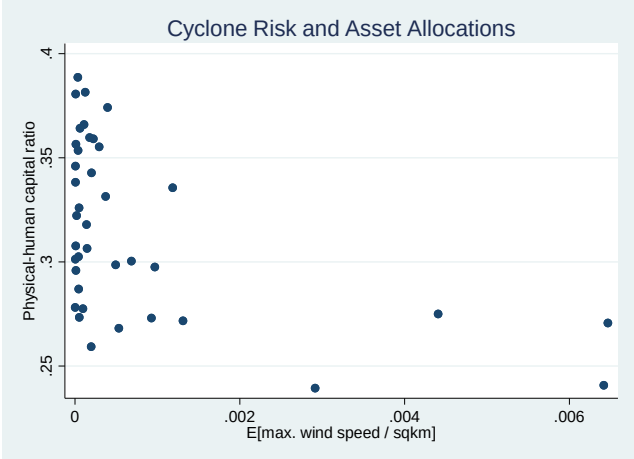

Figure A11: Cyclone Risk and Asset Allocations

References

[1] Barro, Robert J., and Jong Wha Lee. "A new data set of educational attainment in the world, 1950–2010." Journal of development economics 104 (2012): 184-198.

[2] Neumayer, Eric, Thomas Plümper, and Fabian Barthel. "The political economy of natural disaster damage." Global Environmental Change 24 (2014): 8-19.

[3] Emanuel, Kerry A. "Downscaling CMIP5 climate models shows increased tropical cyclone activity over the 21st century." Proceedings of the National Academy of Sciences 110, no. 30 (2013): 12219-12224.

[4] Emanuel, Kerry, Ragoth Sundararajan, and John Williams. "Hurricanes and global warming: Results from downscaling IPCC AR4 simulations." Bulletin of the American Meteorological Society 89.3 (2008): 347-368.

[5] GFDL (Geophysical Fluid Dynamics Laboratory). "Global Warming and Hurricanes." [Accessed 07/02/2018]: https://www.gfdl.noaa.gov/global-warming-and-hurricanes/

[6] Holland, Greg, and Cindy L. Bruyère. "Recent intense hurricane response to global climate change." Climate Dynamics 42, no. 3-4 (2014): 617-627.

[7] IPCC Solomon, S., D. Qin, M. Manning, Z. Chen, M. Marquis, K.B. Averyt, M. Tignor and H.L. Miller (eds.) *Contribution of Working Group I to the Fourth Assessment Report of the Intergovernmental Panel on Climate Change*, Cambridge University Press, Cambridge, United Kingdom and New York, NY, USA. (2007).

[8] Krebs, Tom. "Human capital risk and economic growth." The Quarterly Journal of Economics 118, no. 2 (2003a): 709-744.

[9] Krebs, Tom. "Growth and welfare effects of business cycles in economies with idiosyncratic human capital risk." Review of Economic Dynamics 6, no. 4 (2003b): 846-868.

[10] Rubel, F., and M. Kottek, "Observed and projected climate shifts 1901-2100 depicted by world maps of the Köppen-Geiger climate classification." Meteorol. Z., 19 (2010): 135-141.